JOURNAL OF SYNCHROTRON RADIATION
ISSN 1600-5775

On obtaining high spectral resolution in extreme ultraviolet/soft X-ray monochromators operating off-plane diffraction in a divergent incident beam

Werner Jark*

Elettra – Sincrotrone Trieste SCpA, SS 14 – km 163.5 in AREA Science Park, Basovizza, Trieste 34149, Italy.
*Correspondence e-mail: jark@elettra.eu

Received 9 April 2020
Accepted 15 August 2020

Edited by M. Yabashi, RIKEN SPring-8 Center, Japan

Keywords: diffraction grating; aberrations; off-plane diffraction; extreme ultraviolet; soft X-rays; monochromators.

When the trajectory of an incident beam is oriented parallel to the grooves of a periodic grating structure the radiation beam is diffracted off-plane orthogonal to the plane of incidence. The diffraction efficiency in this condition is very high and in a grating with a sawtooth profile it can approach the reflection coefficient for a simple mirror, when the diffraction order of interest follows the direction for specular reflection at the flat part of the steps. When this concept is used in a plane grating in a monochromator for synchrotron radiation sources, the incident beam is almost always collimated in order to minimize any deterioration of the beam properties due to aberrations, which will be introduced in the diffraction process when an uncollimated beam is used. These aberrations are very severe when the groove density is constant. It will be shown that the effect of these aberrations can be corrected after the diffraction by the use of astigmatic focusing. The latter can be provided by a crossed mirror pair with different focal lengths in the corresponding orthogonal directions. Then a monochromator based on this concept can provide source size limited spectral resolution in an uncollimated incident beam. This is identical to the spectral resolution that can be provided by the same grating when operated at the same position in a collimated incident beam. The source size limited spectral resolution in this case corresponds to a high spectral resolving power of better than $\Delta E/E = 10\,000$ for photon energies around 300 eV in the soft X-ray range.

1. Introduction

Off-plane diffraction from a reflection grating occurs when the trajectory of the incident beam is almost parallel to the grating grooves. Then, as proposed by Greig & Ferguson (1950) for infrared radiation and later repeated by Werner (1977) for soft X-rays, a very special condition can be realized in reflection gratings with a staircase profile. In fact, in this case the direction of the diffracted beam of interest can be made to correspond to the direction of the specularly reflected beam from the flat tops of the stairs. This situation is depicted in Fig. 1 for the lower diffracted beam and it is referred to as the blaze-maximum configuration. Soft X-rays are reflected appreciably only at very shallow grazing angles (see, for example, Werner, 1977) and in this condition the inactive antiblaze part of rectangular steps will not introduce any shadowing into the diffracted beam. Then the grating looks like a system of parallel micro-mirrors and consequently one expects to find diffraction efficiencies which, according to predictions by Nevière *et al.* (1978) and Vincent *et al.* (1979), can ultimately be almost identical to the specular reflection coefficient for a mirror operated with the same simple coating and at the same angle of grazing incidence.

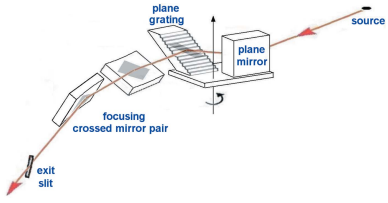

Such comparably high diffraction efficiency is presently mostly considered when a high instrumental transmission is mandatory. The most notable applications in this respect are in spectrometers to be used in space science as proposed, for example, by Cash (1982, 1987, 1991) and by McEntaffer (2019), when weak soft X-ray sources are the target of the investigation, and when two or more gratings need to be arranged in a tandem configuration in an optical instrument. The combined use of two gratings is proposed by Poletto *et al.* (2009) to be used in a time compensation scheme, when the length of short pulses emitted from laser sources in the extreme ultraviolet (EUV)/soft X-ray range is not to be increased in the beam transport system. This could be achieved as reported by Lucchini *et al.* (2018). As far as the production of the related gratings is concerned, the space science community makes the most significant efforts in this respect as reported by McEntaffer (2019). In fact, the use of many identical gratings has been proposed in off-plane diffraction in spectrographs with a larger collection area to be sent into space (*e.g.* Cash, 1991; McEntaffer, 2019). Recently, using state-of-the-art production technology to produce master structures of high quality for the grating replication process, very promising performance was experimentally verified at prototype structures by Miles *et al.* (2018) and by McCoy *et al.* (2020) for the soft X-ray range. The measurements concerned photon energies from 200 eV up to 1200 eV. Unlike at a synchrotron, in space science one finds the sources at infinity, and then as shown by Cash (1983) the removal of the principal aberration in the diffraction process can be achieved in the grating structure by linearly varying the groove separation along the beam footprint in so-called radial groove gratings. The latest study by McCoy *et al.* (2020) considers the production of such radial groove gratings. Instead Miles *et al.* (2018) concentrated on the use of wet anisotropic etching into monocrystalline silicon. This technique allows the production of sawtooth facets, which are atomically flat; however, the technique is not compatible with the concept of radial groove gratings. Miles *et al.* (2018) used such structures as a master for the replication of grating structures with a rather large blaze angle. For these structures they found the best relative efficiency performance reported up to now for the chosen photon energies in the soft X-ray range. The data were measured for a step inclination, or blaze angle, of $\delta = 29.5^\circ$ in a gold (Au)-coated grating with a large groove density of 6250 mm^{-1} for several diffraction orders. The absolute diffraction efficiencies measured at very shallow grazing incidence ($<2^\circ$) varied in this case between more than 60% in the first order at 400 eV photon energy and more than 35% in the fourth order at about 1150 eV photon energy. This is a relative performance of up to 90% and at least 50% of the corresponding mirror reflectivities. Such efficient performance has not yet been reported in the indicated spectral range for any other grating profile or orientation. Consequently the present study considers the use of blazed gratings produced in this way.

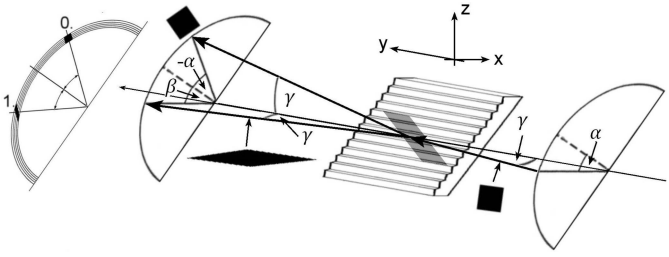

Figure 1
Schematic for the positioning of a plane grating with a staircase profile in the Cartesian laboratory system such that the incident and the off-plane diffracted beam progress in the horizontal x–y plane from right to left. The diffraction takes place in the blaze-maximum condition, *i.e.* the direction for the diffracted beam corresponds to specular reflection at the top of the stairs. The two half arcs next to the grating refer to the cones with identical opening angle γ on which the incident beam and all diffracted orders will be found. The angle α indicates the orientation angle for the incident beam and for the beam which is specularly reflected at the grating surface, *i.e.* for the beam diffracted in zeroth order. This angle is referenced with respect to the nominal plane of incidence defined by the dashed lines in the arcs. The angle β refers to the orientation of a beam which is diffracted in blaze maximum. Black squares and parallelograms attached to different positions in the beam trajectories illustrate the respective cross sections of the beam. The grey parallelogram presents the related footprint at the grating. The detached arc at the left indicates how the grating equation (1) will affect the residual divergences of the incident beam upon diffraction into the zeroth and the first diffraction order as explained by Cash (1982) (see text for a more detailed explanation).

When the operation of a reflection grating in a monochromator for soft X-rays at a synchrotron radiation source is concerned, the off-plane diffraction is notorious for providing only moderate spectral resolution inferior to what is feasible in in-plane diffraction (see *e.g.* Werner & Visser, 1981). Frassetto *et al.* (2008) and Poletto & Frassetto (2009) were the first to propose that this problem can be overcome when rather high diffraction orders are utilized in blaze maximum in off-plane diffraction from gratings with rather large blaze angles. The related instrument is projected for tuning at photon energies around 120 eV and is thus operated at steeper angles of grazing incidence. Jark (2020) discussed recently that this operation scheme can be extended into the soft X-ray range up to photon energies of 2000 eV by utilizing the grating tested by Miles *et al.* (2018) at smaller angles of grazing incidence. Now, the commonly operated optical configuration for monochromators using off-plane diffraction in combination with synchrotron radiation is based on a beam collimation upstream of the grating (see *e.g.* Frassetto *et al.*, 2011, 2014), which was proposed earlier by Werner & Visser (1981). The beam collimation will avoid any performance deterioration due to the aberrations which would otherwise be introduced in the diffraction process. Then, downstream of the grating a focusing mirror in combination with an exit slit serves for the selection of the photon energy of the monochromatic beam. It has also been proposed that the latter two mirrors are installed in the monochromator (Jark, 2020), which is presented here in Fig. 2. In the latter concept an additional plane mirror upstream of the grating, and rotated simultaneously with it, permits continuous tuning in blaze maximum, and thus with high instrumental transmission, from the EUV spectral range at 30 eV photon energy up to 2000 eV in the soft X-ray range.

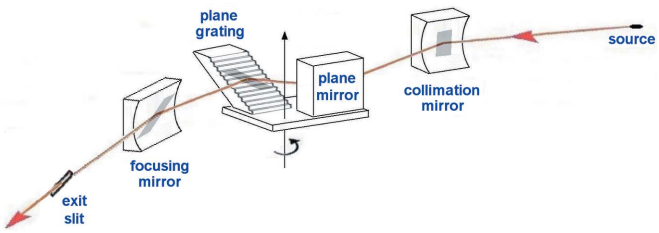

Figure 2
Proposed scheme for an optical configuration for a grazing-incidence monochromator in which a plane mirror/grating pair will diffract a collimated beam in blaze-maximum mode in off-plane diffraction in the horizontal direction. According to Jark (2020) a combined rotation of the plane mirror and the grating around a fixed axis is feasible, and the arrow indicates the direction for increasing the photon energy. The grey areas at the optical components indicate the shape of the beam footprints (see Fig. 1).

Jark (2020) showed that this concept can provide competitive spectral resolving powers of the order of 10 000 or better when the monochromator is installed at undulators at state-of-the-art synchrotron radiation sources. The feasibility of mounting the plane mirror and the plane grating in a fixed orientation with respect to each other, as shown in Fig. 2, is discussed by Jark (2020). This provides interesting advantageous features for the stability of the diffracted beam, when compared with monochromators utilizing in-plane diffraction in the vertical laboratory direction. In fact, the use of a rigidly connected mirror–grating pair will make the position and the direction of the diffracted beam mostly immune to vibrations in the mechanical unit. This applies to vibrations in the horizontal direction and especially in the vertical direction, which may be introduced by an occasionally vibrating laboratory floor.

In the off-plane diffracting systems discussed so far, the two peripheral mirrors need to collimate or focus the beam in both directions and they have thus to be produced with more complicated concave surfaces. In the time compensation scheme proposed by Poletto *et al.* (2009) even four such mirrors are needed. One is thus tempted to ask whether some of these mirrors, which have very demanding tolerances with respect to the fabrication and alignment, can eventually be eliminated or substituted by mirrors of a simpler shape. Consequently, the present study will address the question of whether or not the spectral resolution of the monochromator can be maintained when the beam collimation is abandoned.

2. Theoretical considerations

2.1. Grating equation for off-plane diffraction in the blaze-maximum condition

Werner (1977) showed that in off-plane diffraction the incident beam and all permitted diffraction orders for a particular photon energy are found on symmetric circular double cones as shown in Fig. 1. The cone opening angle γ is counted with respect to the symmetry axis. The latter lies in this case in the grating surface and is parallel to the grooves as illustrated in Fig. 1. This particular orientation of the diffracted orders also gave rise to the description of the geometry as conical diffraction. The grating equation for this orientation, which is generally valid, was derived in radial coordinates by Werner (1977) as

$$\frac{m\lambda}{d} = \sin\gamma\,(\sin\alpha + \sin\beta). \tag{1}$$

Here λ is the wavelength of the monochromated radiation of order number m, d is the groove separation in the grating, and α and β are the orientation angles for the incident and the diffracted beam on the cone with respect to the normal to the grating surface, respectively. The groove density D_0 is then the reciprocal of the groove spacing $D_0 = 1/d$. The wavelength λ and the photon energy E are related via E (eV) = 1239.852/λ (nm). α and β will have the same sign when the incident and the diffracted rays are found on the same side of the plane, which is spanned by the surface normal and the cone axis. As pointed out by Cash (1982), the two products ($\sin\gamma\sin\alpha$) and ($\sin\gamma\sin\beta$) in equation (1) are then simply the projections of the orientation of the latter two beams onto the horizontal axis. According to Cash (1982), the tracing of rays through the system is then particularly simple as, according to equation (1), the sum of both projections is directly related to the monochromated wavelength λ. Now the diffraction in blaze maximum refers in Fig. 1 to the diffracted beam, which is inclined by the angle β with respect to the plane containing the normal to the grating surface. Then in blaze maximum for a grating with a blaze angle of δ one finds $\beta = \alpha = \delta$ and thus

$$\frac{m\lambda_{\rm blaze}}{d} = 2\sin\gamma\sin\alpha = 2\sin\gamma\sin\delta. \tag{2}$$

This study will now deal exclusively with the blaze-maximum condition, *i.e.* the use of the fixed orientation angle $\alpha = \delta$ is considered. Then for the tuning in a monochromator according to equation (2) one has to vary the cone angle γ. This should preferably be done by keeping the diffracted beam stationary in position and in direction. A technical solution for this condition has already been proposed by Werner & Visser (1981). It is proposed that the grating is operated between two plane mirrors, which during tuning will simultaneously rotate in opposite directions, while the grating is translated perpendicular to the undeflected beam trajectory. This three-bounce concept requires a complicated mechanical configuration. Thus Jark (2020) showed that the blaze-maximum condition can also be kept when only one plane mirror is rotated simultaneously with the grating. This significantly simpler system is presented in Fig. 2. Neither of these solutions is used in currently operated off-plane diffracting monochromators (Frassetto *et al.*, 2011, 2014). Instead, in these instruments the simplest solution for the tuning is applied, *i.e.* the grating orientation angle α is varied by simply rolling the grating around the incident beam. Then the grating is operated in blaze maximum only at a particular photon energy and at integer multiples of it. The present findings can then only be applied in the latter condition.

2.2. Aberrations in off-plane diffraction

At a synchrotron radiation source the beam size is usually the smallest in the vertical direction and thus the off-plane diffraction is now assumed to take place in the vertical plane. The strategy is for keeping the diffracted beam in the horizontal plane. Consequently diffraction in the blaze-maximum condition is obtained when the grating is inclined by the groove inclination angle, *i.e.* by the angle $\alpha = \beta = \delta$, with respect to the vertical plane. Then neither the incident nor the diffracted beam will be found in the symmetry plane for the cones, *i.e.* in the plane which is orthogonal to the grating surface and which contains the dashed radius vectors of the cones in Fig. 1. This latter grating orientation now introduces several aberrations into the diffracted beam. These will be studied here for a divergent beam, *i.e.* for an unfocused beam originating from a small source at a finite distance Y_0 upstream of the grating. A finite rectangular aperture just upstream of the grating with sizes A_x and A_z in the Cartesian laboratory coordinate system will then accept a beam with angular spreads of $\Delta A_x = A_x/Y_0$ and of $\Delta A_z = A_z/Y_0$. The latter angular spreads will be limited to the small opening angles of the emission cone according to the considerations of Coisson (1988) relating to the optimum flux collection at an undulator at a storage ring. Superimposed onto the latter angular spread is the intrinsic beam divergence given by the finite source size s.

The consequences of all beam divergences are schematically illustrated in Fig. 1. The beam passing the rectangular aperture just upstream of the inclined grating will produce a footprint at the grating with the shape of a parallelogram as indicated by the grey shadow at the grating in Fig. 1 and Fig. 2. The outline of this footprint for the example case $\alpha = 29.5^\circ$ is shown in Fig. 3. After the diffraction the cross section of the specularly reflected beam, *i.e.* of the zeroth diffraction order,

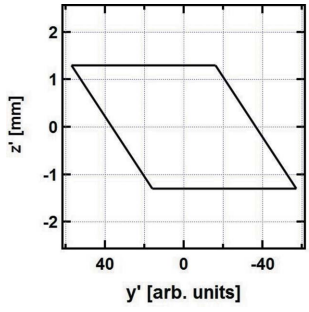

Figure 3
Outline of the beam footprint at the grating in coordinates y'–z', which refer to the grating surface, in the condition presented in Figs. 1 and 2, when the beam passes an aperture with a square shape and side length of 2.2 mm just upstream of the grating. The figure applies for a grating surface inclination by the blaze angle $\delta = 29.5^\circ$ with respect to the vertical direction in the laboratory. The inclinations between the sides of the parallelogram do not vary with the angle of grazing incidence for the incident beam. The unit of the abscissa for the presented outline is mm when a grating with a groove density of 6250 mm^{-1} is operated at an opening angle of the cone of $\gamma = 31.732$ mrad (1.818°). Then according to equation (2) the integer multiples of the fundamental photon energy of 248 eV (wavelength $\lambda = 5$ nm), *i.e.* also 496 eV ($m = 2$), 744 eV ($m = 3$), 992 eV ($m = 4$), are diffracted in the blaze-maximum condition.

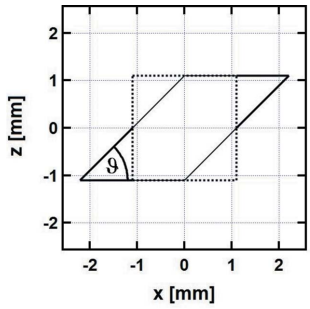

Figure 4
Comparison of the beam cross sections around the grating in the condition presented in Figs. 1–3. The solid line presents the cross section just downstream of the grating upon off-plane diffraction for an incident beam, which passed an aperture with square shape (dashed line) just upstream of the grating. The figure applies for a staircase inclination of $\alpha = 29.5^\circ$ and the parallelogram inclination angle ϑ is calculated by using equation (3).

will be of unaltered rectangular shape, though its orientation with respect to the plane of incidence is reversed. On the other hand, the cross section of the off-plane diffracted beam will be of parallelogram shape as shown in Fig. 4. It should be noted that the orientation at the latter parallelogram is reversed with respect to the footprint and that it is sheared twice more. The shearing angle ϑ in the latter diffracted beam is given by

$$\tan\vartheta = \frac{1}{2\sin\alpha}. \tag{3}$$

Then the shearing increases with increasing inclination angle α and is thus not very significant for smaller angles α.

2.2.1. Variation of the intrinsic beam divergence. In the arc presented at the left in Fig. 1 the effect of the off-plane diffraction on the finite intrinsic beam divergences is indicated. This argument has been discussed in much detail by Cash (1982) and the underlying ray-tracing can be made by use of the general grating equation (1). For the purpose of this study the effect can best be understood by ray-tracing the diffracted beam back towards the original source position. More generally, from now on the matter of discussion will be the virtual coordinates of any diffracted ray of a given wavelength upstream of the grating. This procedure will then be referred to as back-tracing. As discussed by Cash (1982) and shown in Fig. 1, the back-traced diffracted rays for a source with rectangular shape form a virtual source approximately with the shape of a parallelogram. For the purpose of the present discussion, the very small curvature which the conical diffraction adds to all sides of the parallelogram can be neglected. The source is here assumed to be of rectangular shape with height $a = 50$ µm and width $b = 100$ µm and with constant emission point density. When back-traced to the original source position the lengths of the two sides a and b of the parallelogram, as presented in Fig. 5, remain unchanged, while, as was derived by Cash (1982), the longer side is now inclined with respect to the vertical axis by

$$\tan\varphi = \frac{1}{2\tan\alpha}. \tag{4}$$

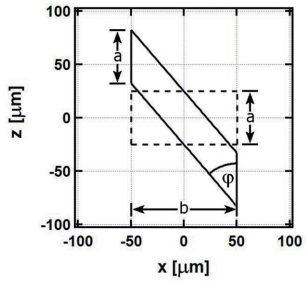

Figure 5
Comparison between the cross section of a rectangular source with height $a = 50$ μm and width $b = 100$ μm (outlined with dashed lines) and its back-traced virtual appearance (outlined with solid lines) at the original source position after off-plane diffraction in the condition presented in Figs. 1–4. The diffraction is assumed to have taken place in a single point at the grating for which an inclination of its surface by $\alpha = 29.5°$ is assumed. Both cross sections are plotted symmetrically with respect to their centres. The angle φ is the inclination angle between the sides of the parallelogram according to equation (4).

Again, as in equation (3), the shearing increases with increasing inclination angle α, but now in the vertical instead of the horizontal direction and with a slightly larger slope. The parallelogram in Fig. 5 then presents the distribution of the intrinsic divergences of the diffracted beam in the Cartesian laboratory system. These intrinsic divergences still apply to any diffracted beam regardless of whether the incident beam is divergent or collimated. By using them one can calculate the related beam blur of a virtual beam cross section upstream of the grating as well as the beam cross section up to the next downstream optics. These intrinsic divergences will not be altered when reflecting optical components of perfect shape are employed downstream of the grating. In any case, here all components will be assumed to be of perfect shape and without imperfections from the manufacturing process. Then the final monochromatic image of the source in the focal plane of the monochromator will be a parallelogram of identical or eventually reversed shape. In the scheme presented here the monochromatic image will then be inclined in the Cartesian laboratory frame.

2.2.2. Conical diffraction at grazing incidence at a 'thick grating'. Cash (1983) also discusses another significant aberration arising in off-plane diffraction, the 'thick optics' case. This is best understood by considering a beam arising from a point source with an angular spread only in the horizontal x direction. In the configuration as presented in Fig. 1 it will then illuminate just one groove from which it will be diffracted off-plane in the vertical z direction by an angle which is constant along the entire footprint. As shown by Cash (1983) this will widen the narrow line in the vertical direction depending on the length of the footprint. This aberration arises from the fact that the grating is a 'thick optics' in the direction of the beam trajectory. When a point source is assumed, this aberration will lead to a back-traced virtual source at the original source position Y_0 upstream of the grating ($Y_0 < 0$) with a vertically increased size as discussed by Jark (2016) and given by

$$a_z = \frac{m\lambda}{d}\frac{\Delta A_x}{\sin\gamma\cos\alpha}|Y_0|. \tag{5}$$

On the one hand, this beam broadening can be ignored when the incident beam is collimated, *i.e.* when the angular spread in the incident beam, or its divergence, ΔA_x, is negligible. On the other hand, this aberration can be eliminated for a divergent incident beam as shown by Cash (1983) when the groove density is made to vary radially along the beam trajectory with all groove axes pointing to the centre of the source.

2.2.3. Deformation of the beam cross section. It was previously not discussed that the deformation of the beam cross section from a beam with rectangular shape to the parallelogram shape adds another very severe aberration to a divergent beam. This is best understood by considering again a beam arising from a point source but now with an angular spread only in the vertical z direction. Such a line beam illuminates a line footprint, *i.e.* an infinitely thin parallelogram of which the longer side is inclined with respect to the grooves. As a consequence, the diffracted beam is then an even more sheared parallelogram, which is inclined with respect to the incident line. The extent of the diffracted line in the horizontal direction is then

$$a_x = 2A_z\tan\alpha, \tag{6}$$

which is a constant. Even when back-traced to the original source position, the virtual line beam will maintain this extent in the horizontal direction.

3. Discussion

3.1. Minimization of the effect of the aberrations in a divergent incident beam

Here it will now be analysed whether the deteriorating effect of the latter two aberrations discussed in Sections 2.2.2 and 2.2.3 can be circumvented in some way, when a grating with constant groove density is operated in a divergent incident beam. Now Y will indicate the distance of an observation point in the beam direction from the grating, with $Y > 0$ being associated with the diffracted ray and $Y < 0$ referring to the back-traced virtual path. Then, on the one hand, the vertically most inclined ray on the optical axis of the system would have passed at $Y = 0$ the coordinates $[x_v(Y = 0), z_v(Y = 0)] = [0, A_z/2]$. Due to the grating inclination the related diffracted ray will follow the path

$$[x_v, z_v] = \left[A_z\tan\alpha, \frac{A_z}{2}\left(\frac{Y_0 - Y}{Y_0}\right)\right]. \tag{7}$$

The orientation angle of the indicated path in the laboratory frame and with respect to the optical axis (0,0) varies then along the beam path and is given by

$$\tan\theta_v = \frac{z_v}{x_v} = \left(\frac{Y_0 - Y}{Y_0}\right)\frac{1}{2\tan\alpha}. \tag{8}$$

The latter inclination now applies to all rays emitted on the optical axis only with a vertical offset. These rays will thus always be found on a line, which is inclined as given by equation (8).

Now, on the other hand, the horizontally most inclined ray on the optical axis of the system is diffracted at the grating at the coordinate $[A_x/2,0]$. According to equation (5) its coordinates in the virtual source at the original source position are

$$\left[0, \frac{m\lambda}{d}\frac{\Delta A_x}{\sin\gamma\cos\alpha}Y_0\right].$$

Then with the angular spread of the beam in the horizontal direction of $\Delta A_x = A_x/Y_0$ its path is given by

$$\left[x_h, z_h\right] = \left[\frac{1}{2}\frac{A_x}{Y_0}(Y_0 - Y), \frac{1}{2}\frac{m\lambda}{d}\frac{A_x}{\sin\gamma\cos\alpha}\left(\frac{Y}{Y_0}\right)\right]. \quad (9)$$

In this case the orientation angle of the indicated ray in the laboratory frame and with respect to the optical axis is

$$\tan\theta_h = \frac{z_h}{x_h} = \frac{m\lambda}{d}\frac{1}{\sin\gamma\cos\alpha}\frac{Y}{(Y_0 - Y)}. \quad (10)$$

Also here the latter inclination applies to all rays emitted vertically on the optical axis only with a horizontal offset. The inclination of the resultant line again varies along the beam path, although differently compared with the inclination according to equation (8).

3.1.1. Virtual sources. As the two inclinations according to equations (8) and (10) vary differently with the distance Y from the grating, it is interesting to investigate the beam properties when both inclinations according to equations (8) and (10) are identical. The latter is the case at two different positions upstream of the grating and thus for virtual beam coordinates Y_1 and Y_2 given by

$$Y_1 = Y_0\left(\frac{1 - \sin\alpha}{\cos\alpha}\right)^2, \quad (11)$$

$$Y_2 = Y_0\left(\frac{1 + \sin\alpha}{\cos\alpha}\right)^2, \quad (12)$$

one then finds

$$Y_1 > Y_0 > Y_2 \quad (13)$$

with

$$Y_1 Y_2 = Y_0^2. \quad (14)$$

According to equations (11) and (12) the two virtual sources upstream of the grating separate in the beam direction even significantly with increasing inclination angle α. Then according to equation (13) the first virtual position falls between the grating and the source, while the second is further away upstream of the real source. The respective inclinations with respect to the horizontal laboratory axis are then

$$\tan\theta_1 = \frac{\cos\alpha}{\sin\alpha + 1} = \frac{1 - \sin\alpha}{\cos\alpha}, \quad (15)$$

$$\tan\theta_2 = \frac{\cos\alpha}{\sin\alpha - 1} = -\frac{1 + \sin\alpha}{\cos\alpha}, \quad (16)$$

which leads to

$$\theta_1 + \theta_2 = -\alpha, \quad (17)$$

$$\theta_1 - \theta_2 = 90^\circ, \quad (18)$$

and thus finally to

$$\theta_1 = \frac{90^\circ - \alpha}{2}, \quad (19)$$

$$\theta_2 = -\frac{90^\circ + \alpha}{2}. \quad (20)$$

3.1.2. Astigmatism in the diffracted beam. When a point source is considered, then the virtual cross sections of the back-traced diffracted beams are simply lines at the indicated positions as per equations (11) and (12). It is now very intriguing that according to equation (18) the latter two lines are always exactly perpendicular with respect to each other. And both the positions, according to equations (11) and (12), and the inclinations, according to equations (19) and (20), of the virtual sources remain stationary as long as the grating is operated in blaze-maximum mode, *i.e.* for constant inclination $\alpha = \delta$. Consequently the off-plane diffraction introduces a very simple form of astigmatism into the diffracted beam with two longitudinally well separated virtual sources, which are orthogonal with respect to each other. In order to create images of both virtual sources at the same position downstream of the grating the diffracted beam then needs to be focused utilizing astigmatic focusing. The latter can be provided by the use of a simple astigmatic mirror focusing bi-dimensionally with different focal lengths in orthogonal directions. Alternatively also a crossed pair of orthogonal one-dimensionally focusing mirrors, as proposed for the focusing of X-rays by Kirkpatrick & Baez (1948), can be used. The choice of the more appropriate solution now depends on whether or not the direction of the smaller extent of one of the virtual line sources coincides with the dispersion direction of the grating. In Fig. 1 one finds that the wavelength dispersion in off-plane diffraction in the indicated grating orientation is provided in the laboratory frame in the vertical direction. The dispersion direction and the direction of the smaller extent in one of the virtual sources will be identical only when one of the two inclination angles according to equations (19) or (20) is equal to 0°. Now for reasonable orientation angles with $\alpha <$ 45° the first inclination θ_1 varies according to equation (19) in the range $22.5^\circ < \theta_1 < 45^\circ$. Then neither this virtual source nor the orthogonal other source are ever close to being horizontal in the laboratory frame. Consequently, when the incident beam has a larger bandwidth, both back-traced lines will be broadened by the dispersion.

A similar observation is not made in classical in-plane diffraction, *i.e.* when $\gamma = 90^\circ$ in equation (1). Also in the latter case the diffraction will introduce astigmatism into a divergent incident beam. This argument is discussed by Petersen (1982) in investigating the defocus aberration (see *e.g.* Beutler, 1945; Werner, 1967) in in-plane diffraction. The result is a virtual source in the plane of incidence upstream of the grating at a different position compared with the real source position. Instead, in the orthogonal direction the virtual and the real source position will still coincide. Consequently the diffracted

beam is astigmatic; however, only the virtual source in the dispersion direction of the grating is dispersion broadened. This broadening varies linearly with the source size, and the dispersion direction is thus chosen to coincide with the direction of the smaller source dimension. Then it is sufficient for the wavelength selection with optimum spectral resolution, *i.e.* with the source size limit, to discriminate a given diffraction direction by focusing only the dispersion-broadened virtual source into an exit slit. The focusing in the orthogonal direction is not required. The monochromatic image in the exit slit is then a longer line, as discussed by Reininger & Saile (1990). However, practically the independent focusing in the orthogonal direction is almost always used in monochromators, which are operated at smaller sources, in order to maximize the photon density in the exit slit.

Instead, in the system discussed here, the proper focusing of both dispersion-broadened virtual sources is mandatory when the optimum source size limited spectral resolution is to be achieved. The proper focusing will be practically very difficult or even impossible to realize by the use of a single mirror, considering reasonable fabrication tolerances for the production of the related mirror, *e.g.* a toroidal mirror with different focal lengths in the tangential and the sagittal direction. In this respect a pair of crossed mirrors, commonly referred to as KB mirrors (Kirkpatrick & Baez, 1948), which can be aligned independently in the two relevant directions, offers much more flexibility.

3.1.3. Broadening of the virtual sources due to the intrinsic source size limited beam divergences. The deformation of the originally rectangular divergence plot to an inclined parallelogram, as shown in Fig. 5, seems to offer the possibility of providing very narrow virtual lines: the resultant intrinsic beam divergence is the smallest in an inclined direction, where it is even smaller than the intrinsic beam divergence in the direction of the smaller source dimension. One could then make optimal use of this if the inclination of one of the two virtual line sources could be matched to the inclination of the divergence parallelogram. Obviously, only the line inclined by the angle θ_2 can have a similar inclination. Its corresponding inclination with respect to the vertical axis can be made identical to the inclination angle according to equation (4) only towards the limit of $\alpha = 90^\circ$ for the orientation angle. This is not a reasonable inclination or blaze angle. Nevertheless, an appreciable divergence reduction effect is still available in combination with larger feasible blaze angles. For the reasonable limit of $\delta = 45^\circ$ the mismatch between the two relevant angles φ and θ_1 is rather small with $\varphi = 26.57^\circ$ and a line inclination of $\theta_1 = 22.5^\circ$. And even for the value of δ chosen here, $\delta = 29.5^\circ$, the corresponding numbers of $\varphi = 41.47^\circ$ and a line inclination of $\theta_1 = 30.25^\circ$ result in a slightly larger, though still favourable, mismatch. In any case, the residual beam divergence to be applied to the two virtual sources is given by the projection of the divergence parallelogram onto the directions orthogonal to the virtual lines. Then, while the farther virtual line source will be minimally blurred, the closer virtual line source instead will be significantly blurred. In this case the blur is dominated by the larger intrinsic divergence, which the off-plane diffraction introduces in the respective direction, and which is originated by the larger horizontal source size.

3.2. Verification of the predicted virtual sources by the use of ray-tracing calculations

The arguments just presented are now discussed for a grating with the large blaze angle of $\delta = 29.5^\circ$, which has already been successfully prepared by Miles *et al.* (2018). This grating has a groove density of $D_0 = 6250\ \text{mm}^{-1}$ and it is positioned for the parameters as shown in Figs. 3–5, *i.e.* the angle of grazing incidence onto the flat stairs of the grating profile is $\gamma = 31.732$ mrad (1.818°), which provides first-order diffraction for 248 eV photon energy. The source is of rectangular shape with constant photon density and with height $a = 50$ µm and width $b = 100$ µm. This height corresponds to the full width at half-maximum of the diffraction-limited source size in the vertical direction for the indicated photon energy of 248 eV emitted from a 4.5 m-long undulator (see *e.g.* Jark, 2020). An aperture measuring 2.2 mm × 2.2 mm is illuminated uniformly at a source distance of 22 m just upstream of the grating. Also this angular acceptance corresponds to the opening angle of the emission cone from a 4.5 m-long undulator for 248 eV photon energy. The ray-tracing is performed using the software package *SHADOW* described by Sanchez del Rio *et al.* (2011). In order to identify the dispersion direction and the amount of dispersion a total of four photon energies with different separation of 0.025 eV ($\Delta E/E = 10\,000$) and of 0.05 eV ($\Delta E/E = 5000$) between them are traced, namely 247.975 eV, 248.0 eV, 248.025 eV and 248.075 eV. According to equations (11) and (12) the two orthogonal virtual sources are to be found at the positions $Y_1 = -7.48$ m and $Y_2 = -64.69$ m. The accordingly back-traced spot patterns are presented at the top in Figs. 6 and 7 and confirm the appearance of the two orthogonal line sources. The related lines are inclined in the laboratory frame by $\theta_1 = 30.25^\circ$ and $\theta_2 = -59.75^\circ$ as predicted by the use of equations (19) and (20). In order to more clearly evidence the dispersion, *i.e.* the line broadening and the line separation, the spot patterns presented at the bottom of Figs. 6 and 7 for both virtual sources are rotated such that the dispersion occurs in the vertical display direction.

When one now compares the line inclinations in the upper part of Figs. 6 and 7 with the inclination of the parallelogram presenting the intrinsic beam divergence in Fig. 5, one finds that the virtual line in Fig. 7 is almost parallel to the longer side of the parallelogram, as predicted in Section 3.1.3. The result is a minimal broadening of the single lines, when compared with the line separation, which can be seen in the pattern at the bottom in Fig. 7 for the distant virtual source with inclination $\theta_2 = -59.75^\circ$. Instead, the lines in the pattern at the closer virtual source with inclination $\theta_1 = 30.25^\circ$ at the bottom of Fig. 6 are maximally broadened by the inconveniently large resultant intrinsic divergence perpendicular to the lines.

Now the closer virtual source in Fig. 6 is less inclined with respect to the dispersion direction than the distant source, and consequently the photon energy dispersion in angle, which varies with $\cos\theta$, is larger in this case. In fact, the angular photon energy dispersion is about 1.7-fold larger for θ_1 = 30.25° ($\cos\theta_1$ = 0.864) than it is for θ_2 = −59.75° ($\cos\theta_2$ = 0.504). On the other hand, the line blur introduced by the intrinsic divergence is even fourfold larger for the first angle. As a consequence the lines in the closer virtual source presented at the bottom of Fig. 6 overlap inconveniently significantly, while they are well separated in the distant virtual source presented in Fig. 7, even though the photon energy dispersion is unfavourably smaller in this case.

4. Application of the findings in a soft X-ray monochromator

4.1. Optimization of the optical configuration

In Section 3.1.2 the focusing of the diffracted beam by the use of a crossed mirror pair is favoured. For the moment each mirror will be assumed to focus perfectly in one dimension, which can be achieved with an elliptical surface profile in the tangential direction. Then each of these mirrors can produce at any distance downstream of it a spot pattern with the same ratio between the line width and the line separation as shown at the bottom of Figs. 6 and 7. The lines with a relative separation of $\Delta E/E$ = 10 000 are just separated in Fig. 7 and thus behind a properly positioned exit slit a resolving power of $\Delta E/E$ = 10 000 would be available even when only the farther virtual source is focused. This will require an angle of θ_2 = −59.75° to be applied between the mirror surface and the horizontal direction, and a longer exit slit to be positioned parallel to the mirror surface. In the orthogonal direction the achievable resolving power in the corresponding configuration is obviously much smaller as even the line with a relative separation of $\Delta E/E$ = 5000 is not separated in Fig. 6 from the other lines. Nevertheless, the possibility of achieving independently monochromatization in both orthogonal directions is then very helpful for the alignment of these mirrors. At this point it needs to be investigated how much the achievable spectral resolution can be improved when both focusing mirrors are inserted correctly. Independent of its orientation in rotation around the incident beam a pair of crossed mirrors will not introduce any beam rotation. Consequently, after the related focusing, the direction of the dispersion at the grating will remain unaltered in the vertical direction. Likewise, as argued in Section 2.2.1 with respect to the parallelogram presented in Fig. 5, the final monochromatic image of the

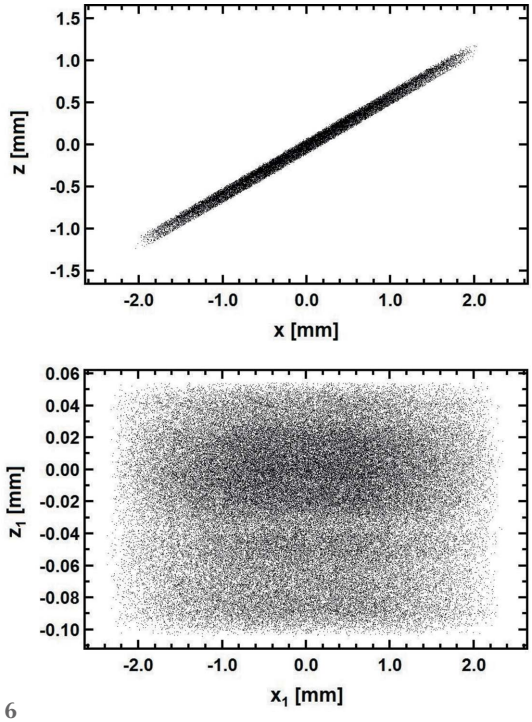

Figure 6
Top: back-traced spot pattern for the diffracted beam at the position of the closer virtual line source according to equation (11) at a distance of Y_1 = −7.48 m upstream of a grating with a groove density of D_0 = 6250 mm^{-1} and a blaze angle of δ = 29.5°. Discrete photon energies of 247.075 eV, 248.0 eV, 248.025 eV and 248.075 eV are progressing at an angle of grazing incidence of γ = 31.732 mrad onto the flat part of the grooves. Bottom: spot pattern from the top after rotation of the window by θ_1 = 30.25° clockwise (100 000 rays).

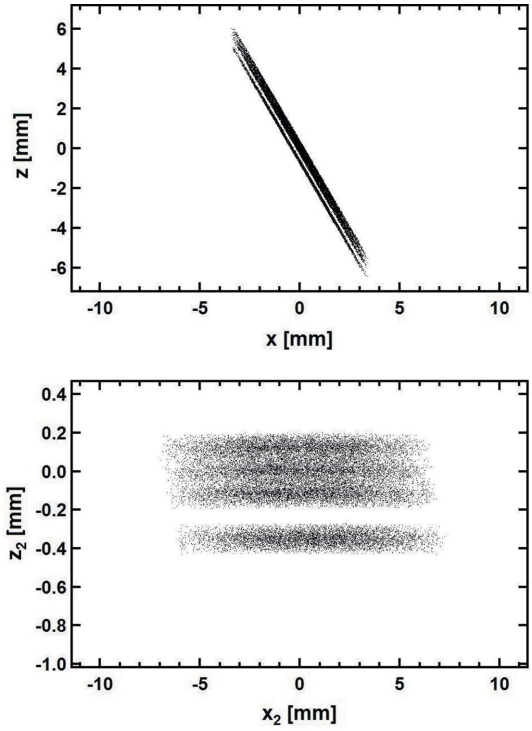

Figure 7
Top: back-traced spot pattern for the diffracted beam at the position of the distant virtual line source according to equation (12) at a distance of Y_2 = −64.69 m upstream of the grating for the parameters reported in Fig. 6. For a comparison with Fig. 6 (top) one has to recognize that the displayed window presents half of the apparent opening angle in comparison with the apparent opening angle of the displayed window in Fig. 6. Bottom: spot pattern from the top after rotation of the window by θ_2 = −59.75°, *i.e.* by 59.75° counterclockwise (25 000 rays). For a comparison of this pattern with the pattern at the bottom of Fig. 6 one has to recognize that both displayed windows present the same apparent opening angle in the vertical direction.

source in the focal plane of the monochromator will be a parallelogram of identical or eventually reversed shape. This will require the photon energy selecting exit slit to be inclined according to equation (4) by an angle $|\varphi| = 41.47^\circ$ with respect to the vertical direction. The rotated orientation of the crossed mirror pair away from a horizontal or vertical positioning is rather unusual. This may be inconvenient for the alignment; however, it provides here an interesting feature as it allows the exiting beam to be kept in a horizontal plane. For this purpose the angles of grazing incidence onto the two mirrors need to be slightly different and the mirrors could be oriented as proposed in the optical scheme in Fig. 8. In this case the mirror closer to the grating reflects the beam upwards towards the reader, while the orthogonal companion deflects it downwards.

The unusual mirror orientation also requires some comments about the possibility that it introduces polarization effects. The incident beam is linearly polarized with the electric field vector in the horizontal plane. Then, in each reflection process in which the beam is not deflected exclusively in the horizontal or in the vertical direction the electric field amplitude will be split into two orthogonal components, one parallel to the surface and the other perpendicular to it. Polarization effects will then only be found (*e.g.* Born & Wolf, 1980) when the reflection coefficients for the two components are appreciably different and/or when the phase retardation between the two reflected components is significantly different from 0 or π. In the first case the electric field vector will be rotated with respect to the incident beam, while in the second case the electric field vector will start to rotate, giving rise to the progression of elliptically and eventually circularly polarized light. According to Marlowe *et al.* (2016), a polarization effect has not been found for gratings operated in the off-plane configuration in the soft X-ray range considered here. Kortright & Underwood (1990) showed that significantly different reflection coefficients and phase shifts different from π will not be found at rather small grazing angles, but in the vicinity of the Brewster angle, which in this case for soft X-rays occurs at a larger angle of grazing incidence of about 45°. Here the angles of grazing incidence onto the crossed mirror pair will be fixed and they will be chosen to be small, of the order of 1°, in order to provide high reflectivity up to a photon energy of 2000 eV. In this condition this pair will thus not alter the polarization state of the incident beam. Only this pair could eventually give rise to elliptically polarized light, while the reflection at the vertical surface of the plane mirror upstream of the grating keeps the electric field vector of the incident linearly polarized light in the horizontal plane. Then the monochromatic beam will still present the linear polarization of the incident beam.

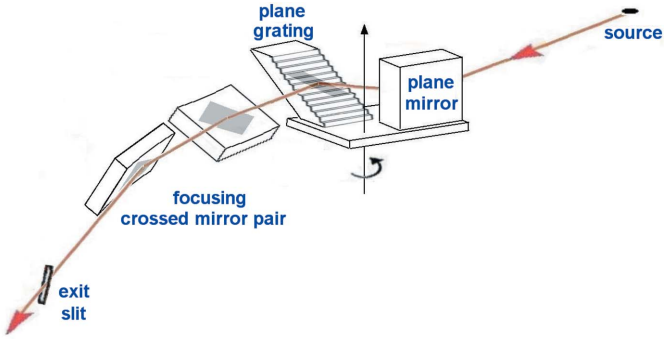

Figure 8
Alternative optical scheme for the monochromator proposal in Fig. 2, which can provide high spectral resolution in blaze-maximum tuning without beam collimation. The aberrations arising in the off-plane diffraction from the plane grating with constant groove density can be eliminated in the divergent beam when an astigmatically focusing crossed mirror pair is operated in an inclined orientation with respect to the laboratory frame. As already indicated in Fig. 2, also here the exit slit needs to be inclined with respect to the vertical direction by the same angle calculated according to equation (4).

4.2. Verification of the performance with ray-tracing calculations for perfect optics

Fig. 9 presents the spot pattern from the ray-tracing in the focal plane for the proposed configuration from Fig. 8 for an image distance of 10 m from the focusing mirrors and for angles of grazing incidence of 1° onto mirrors with elliptical profiles in the tangential directions. The latter distance was chosen to be rather large, in order to avoid the case where the size of the monochromatic image becomes inconveniently small. The pattern in Fig. 9 agrees completely with the expectations discussed in the previous section. One can note that the monochromatic lines in the focal plane are now better separated than the lines in the distant virtual source as presented in Fig. 7. This confirms the need to focus both virtual sources, which each contain dispersion, in order to obtain the ultimate spectral resolving power, which improves then from $\Delta E/E = 10\,000$ for the focusing with only one mirror to values of the order of $\Delta E/E = 14\,000$. The sharpness of the borders of the spot pattern in Fig. 9 indicates that the effect of residual aberrations in the diffracted beam is negligible for the chosen source size. In fact, the latter residual aberrations will

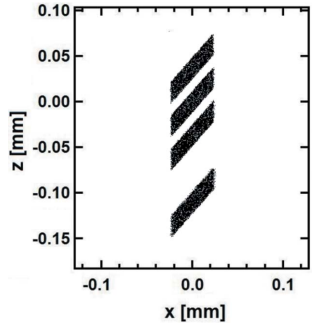

Figure 9
Spot pattern in the focal plane of the monochromator scheme proposed in Fig. 8 with the grating parameters reported in Fig. 6, in which an uncollimated beam is diffracted off-plane and successively focused by the use of an astigmatically focusing crossed mirror pair with different focal length in the orthogonal directions. The latter mirrors are rotated away from a horizontal orientation in the laboratory frame counterclockwise by 30.25° and by 30.25° + 90° for an observer following the beam trajectory.

here start to affect the focus appreciably only when the source is reduced in size tenfold.

The ray-tracing of the collimated setup in Fig. 2 leads, for the same positions for the grating and for the exit slit, to spot patterns of identical shape and size, but with reversed dispersion direction as the diffracted beam is focused then by only one instead of two mirrors. Then identical spectral resolving power can be achieved in both configurations. Consequently, no sacrifice in the obtainable spectral resolution needs to be made when the collimation of the incident beam is abandoned and the grating is thus operated in a divergent incident beam.

4.3. Some practical aspects

The last calculations present 'unusual' aspects for the optimization of a beam transport system, which is based on off-plane diffraction from a plane grating with a rather large blaze angle. These 'unusual' aspects are inherent in the off-plane diffraction process and will thus be found in both presented optical concepts, the collimated incident beam version from Fig. 2 and the uncollimated variant from Fig. 8. First of all, as shown in Fig. 9, the monochromatic images of the source are inclined with respect to the horizontal direction in the plane, in which the exit slit will be positioned. This will require the exit slit to be inclined correspondingly. Secondly, in the diffraction process the beam cross section will be deformed to a parallelogram as presented by the solid line in Fig. 4. Both observations will not be made in monochromators operating with classical in-plane diffraction. In this case the beam cross section and the monochromatic images in the exit slit remain symmetric with respect to the vertical plane of incidence. The question is then whether the beam deformations discussed here present a significant inconvenience. Presently, in almost all monochromators projected for soft X-rays a refocusing mirror will create an image of the exit slit at the sample position. Now any focusing mirror will repeat the image inclination in the exit slit also in the focal plane, and thus here the final focus at the sample will be inclined with respect to the horizontal. When this is not acceptable, then the sample and the detector will have to be mounted in unsual positions.

The diffracted beam will progress in the beam transport system with the deformed cross section of parallelogram shape as presented in Fig. 4. The same shape, albeit with different width and height, will then also be found behind the exit slit at possible positions for the refocusing mirror. Then in order to keep the final focused beam still in the horizontal plane such a refocusing mirror will be operated with a vertical surface. Consequently, the mirror length needs to be matched to the extent of the footprint produced by the beam cross section in the horizontal direction. In order to collect the entire monochromatic beam one will have to double the mirror length compared with the undeformed beam cross section. This is the inconvenience for this aspect. However, one has to recognize that the outermost 50% of an extended mirror length will only collect 25% of the totally available flux. According to Coisson (1988) the opening angle of the emission cone from an undulator will decrease with increasing photon energy, and consequently the length of the footprint of the monochromatic beam at the refocusing mirror will decrease as well. Then the moderate flux loss, when the shorter mirror is chosen, will be found only towards the lower energy limit.

5. Conclusion

It was shown here that the aberrations, which the off-plane diffraction at a plane blazed grating with constant groove density will introduce into an uncollimated incident beam, will make this beam appear like an astigmatic beam. When the grating is operated in a monochromator at a synchrotron radiation source the diffracted beam will appear then as if it had been emitted from two longitudinally well separated virtual line sources at positions different from the real source position. The two lines are orthogonal with respect to each other, and they are inclined in the laboratory frame. These two line sources remain stationary when during the photon energy tuning of the monochromator the diffraction is achieved in the blaze-maximum condition. For the wavelength selection the diffracted beam from a plane grating with constant groove density needs always to be focused into an exit slit. The rather simple astigmatism can then be removed in the latter focusing process by the use of different focal lengths in the two related orthogonal directions, *e.g.* by using an astigmatically focusing crossed mirror pair. In such a configuration the grating chosen here with groove density of $D_0 = 6250\ \text{mm}^{-1}$ and a blaze angle of $\delta = 29.5^\circ$ can then provide source size limited spectral resolving power of the order of $\Delta E/E = 14\,000$, identical to the performance for the grating operation in a collimated incident beam. While the latter system will require two peripheral mirrors of more complex shape, with each providing bi-dimensional focusing, the system described here can provide identical performance by the use of two one-dimensionally focusing mirrors. The first mirrors are curved in both directions and are difficult to manufacture to the correct shape with very tight tolerances as the metrology of the surface figure is then a very demanding and lengthy process. Instead the mirrors in the crossed mirror pair are curved only in the tangential direction. This permits a faster and more accurate metrology, which in turn will make the manufacturing faster and thus cheaper.

References

Beutler, H. G. (1945). *J. Opt. Soc. Am.* **35**, 311–350.
Born, M. & Wolf, E. (1980). *Principle of Optics*, 6th ed. Oxford: Pergamon Press.
Cash, W. (1982). *Appl. Opt.* **21**, 710–717.
Cash, W. (1987). *Appl. Opt.* **26**, 2915–2929.
Cash, W. C. Jr (1983). *Appl. Opt.* **22**, 3971–3976.
Cash, W. C. Jr (1991). *Appl. Opt.* **30**, 1749–1759.
Coisson, R. (1988). *Opt. Eng.* **27**, 273250.
Frassetto, F., Cacho, C., Froud, C. A., Turcu, I. C. E., Villoresi, P., Bryan, W. A., Springate, E. & Poletto, L. (2011). *Opt. Express*, **19**, 19169–19181.
Frassetto, F., Miotti, P. & Poletto, L. (2014). *Photonics*, **1**, 442–454.

Frassetto, F., Poletto, L., Larruquert, J. I. & Mendez, J. A. (2008). *Proc. SPIE*, **7077**, 707712.
Greig, J. H. & Ferguson, W. F. C. (1950). *J. Opt. Soc. Am.* **40**, 504–505.
Jark, W. (2016). *J. Synchrotron Rad.* **23**, 187–195.
Jark, W. (2020). *J. Synchrotron Rad.* **27**, 25–30.
Kirkpatrick, P. & Baez, A. (1948). *J. Opt. Soc. Am.* **38**, 766–774.
Kortright, J. B. & Underwood, J. H. (1990). *Nucl. Instrum. Methods Phys. Res. A*, **291**, 272–277.
Lucchini, M., Lucarelli, G. D., Murari, M., Trabattoni, A., Fabris, N., Frassetto, F., De Silvestri, S., Poletto, L. & Nisoli, M. (2018). *Opt. Express*, **26**, 6771–6784.
Marlowe, H., McEntaffer, R. L., Tutt, J. H., DeRoo, C. T., Miles, D. M., Goray, L. I., Soltwisch, V., Scholze, F., Herrero, A. F. & Laubis, C. (2016). *Appl. Opt.* **55**, 5548–5553.
McCoy, J. A., McEntaffer, R. L. & Miles, D. M. (2020). *Astrophys. J.* **891**, 114.
McEntaffer, R. L. (2019). *J. Astron. Telescopes Instrum. Syst.* **5**, 021002.
Miles, D. M., McCoy, J. A., McEntaffer, R. L., Eichfeld, C. M., Lavallee, G., Labella, M., Drawl, W., Liu, B., DeRoo, C. T. & Steiner, T. (2018). *Astrophys. J.* **869**, 95.
Nevière, M., Maystre, D. & Hunter, W. R. (1978). *J. Opt. Soc. Am.* **68**, 1106–1113.
Petersen, H. (1982). *Opt. Commun.* **40**, 402–406.
Poletto, L. & Frassetto, F. (2009). *Appl. Opt.* **48**, 5363–5370.
Poletto, L., Villoresi, P., Frassetto, F., Calegari, F., Ferrari, F., Lucchini, M., Sansone, G. & Nisoli, M. (2009). *Rev. Sci. Instrum.* **80**, 123109.
Reininger, R. & Saile, V. (1990). *Nucl. Instrum. Methods Phys. Res. A*, **288**, 343–348.
Sanchez del Rio, M., Canestrari, N., Jiang, F. & Cerrina, F. (2011). *J. Synchrotron Rad.* **18**, 708–716.
Vincent, P., Nevière, M. & Maystre, D. (1979). *Appl. Opt.* **18**, 1780–1783.
Werner, W. (1967). *Appl. Opt.* **6**, 1691–1699.
Werner, W. (1977). *Appl. Opt.* **16**, 2078–2080.
Werner, W. & Visser, H. (1981). *Appl. Opt.* **20**, 487–492.